AD A
105930

AD A105930

DTIC FILE COPY

LEVEL II

(11)

(9) Final Report,

to the

(15) Office of Naval Research
Contract No: N00014-79-C-0469

1 JUN 1981 (11) 1979

(6) ACOUSTO-OPTICAL TOMOGRAPHY
INVESTIGATION OF ULTRASONIC FIELD

(12) (17) submitted by

(10) Bill D. Cook
Department of Mechanical Engineering
Cullen College of Engineering
University of Houston Central Campus
Houston, Texas 77004

401241

81 7 16 094

The proposed research was to apply the principles
of computer aid tomography to acousto-optic data for the
purpose of investigating sound radiation and scattering.
The principal investigator had previously developed
the theory and logic but lacked the facilities, namely
for computer acquisition, mass storage, display of the
large amounts of information involved. The objective
of this contract was to allow the principal investigator
and colleagues at the Navy Research Laboratory,
Washington, DC to implement the necessary hardware and
computer algorithms during the semester of 1979. The
Physical Acoustics Branch of the Naval Research Laboratory
had both the acousto-optic facilities and the on-line com-
puter system. Upon submission of the proposal, the
principal investigator sent to the scientific personnel at
NRL, the requirements for the manipulation of the acoustic
radiating system. The personnel there designed a
manipulator and ordered the required parts to build
the device.

The plan of action was for the principal investigator
to become familar with the computer system while the
manipulator was being built. The parts required for the
manipulator were not received during the summer of 1979.

Consequently, the Principal Investigator devoted
himself to theoretical and computational problems of
interest of the Physical Acoustics Branch. The computer

experiments underway at NRL pertaining to acousto-optics
and radiation of sound fields.

ACOUSTO-OPTICS

In as much as tomography may be considered as the
inversion of a scattering process, the Principal Investi-
gator developed an algorithm to calculate the direct
process of scattering of light by ultrasound. The
algorithm is novel in that, one needs only to specify the
nature of radiating acoustic transducer and many of the
observed acousto-optic phenomena can be predicted and
graphically displayed. Attachment A and B are publications
resulting from this activity.

FOCUSED ULTRASONIC FIELDS

An ongoing activity on the Physical Acoustic Branch
of NRL was experimental exploration of focused ultrasonic
fields. The Principal Investigator had recently super-
vised a PhD student on the theory of such fields. A
joint experimental and computational effort was made
to validate the theory. Attachment C is a publication
which shows the success of the activity.

ACOUSTO-OPTIC TOMOGRAPHY

The contract was extended to May 1980 to allow the
Principal Investigator to publish the material and

continue his theoretical investigation at the University
of Houston.   During this period he developed a new
theory of data acquisition for acousto-optic tomography,
trained two undergraduates and submitted a new proposal
to the Office of Naval Research in addition to publishing.
The new proposal was funded by ONR and the two students
and the Principal Investigator returned to NRL for the
Summer of 1980 to continue the research.

A Numerical Procedure for Calculating the Integrated Acoustooptic Effect $\wedge$

BILL D. COOK, SENIOR MEMBER, IEEE, EDUARDO CAVANAGH, AND HENRY D. DARDY, MEMBER, IEEE

Abstract—The integrated optical effect of light passing through an ultrasonic field can be numerically calculated from the velocity distribution assigned to a planar transducer. The theory is developed for linear acoustics, nonabsorbing media, and normal incidence of light. As a consequence of the application of the Fourier projection slice theorem, an algorithm based on digital Fourier transforms calculates the integrated optical effect without integration. Demonstrations of the influence of transducer geometry are shown for the integrated optical effect and schlieren patterns based on this effect.

INTRODUCTION

THE OPTICAL methods for estimating field quantities, such as pressure, of ultrasonic fields required a model of the sound field. Often these were simplistic (collimated plane waves) but very useful. In reality the light usually passes through the near-field region of the ultrasonic transducer. The multitude of schlieren photographs in the literature give testimony to the complexity of the effect of the near field. For example, Fig. 1 shows a schlieren image, published by Osterhammel [1] in 1941, of the near field of a square transducer. The intricate pattern was explained by Osterhammel as interference of planes waves from the face of transducer and circular waves from the edge; this theory does not permit quantitative calculations and is not extendable to other geometries.

Schlieren patterns such as is shown in Fig. 1 can be computed provided the field parameters of the integrated optical effect are known. At low ultrasonic frequencies, the interaction of sound and light can be described by one parameter, the so-called Raman–Nath parameter v [2]. For a three-dimensional pressure field $p(x, y, z) e^{i\omega t}$, with the light traversing in the y direction as shown in Fig. 2, the integrated optical effect is defined as

$$v(x, z) = \frac{2\pi\kappa}{\lambda} \int p(x, y, z)\, dy. \tag{1}$$

Here λ is the optical wavelength and κ is the piezooptic coefficient. The integrated optical effect is thus a two-dimensional phasor field $v(x, z)$. In this paper a computation procedure is presented for calculating $v(x, z)$ when the motion of the transducer is specified. The procedure is straightforward and eased
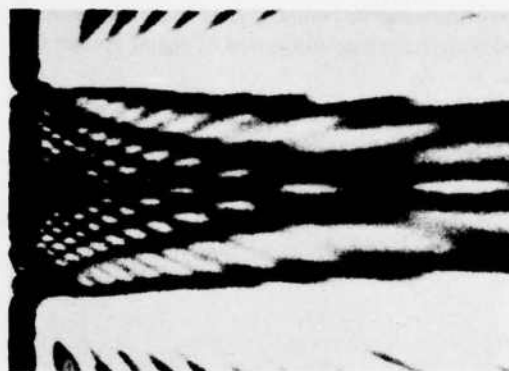

Fig. 1. Schlieren photograph of near field of a square transducer with ratio of width to acoustical wavelength of 14.37, from Osterhammel [1].
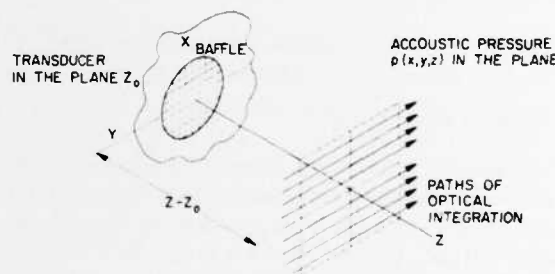

Fig. 2. Diagram showing geometry.

by utilization of the standard one-dimensional Fourier transform which yields the field $v(x, z)$ at a given z as a one-step process.

Analytic solutions and numerical procedures have been attempted on the problem previously. Ingenito and Cook [3] have given an exact formulation for piston-like motions of the transducers with on-axis values given in approximation for a circular, rectangular, and square piston on its diagonal. Maloney, Meltz, and Gravel [4] have treated the square transducer with the Fresnel approximation. Their experimental measurements in solids agreed with theory for both axial and transverse profiles. Crandal [5] also made computations and measurements with emphasis on phase measurements for sound velocity measurements. Haran, Cook, and Stewart [6] have used the theoretical results for comparing optical calibration of a circular transducer with a radiation pressure technique. Riebold *et al.* [7], [8] have also made careful mea-

surements on the axis values to compare with the theory of Igenito and Cook [3]. Berlinghieri and Cook [9] have also calculated the v-field for a circular piston to test an inversion algorithm to estimate the pressure $p(x, y, z)$ from measured values of $v(x, z)$.

The procedure presented here allows calculations throughout the near field including the adjacent region to the transducer where the pressure field and integrated optical effect can vary significantly with a small change of position. The only limitation in calculating the complete field appear to be those connected with the normal utilization of digital Fourier transforms.

THEORY

The procedure that is to be developed is based on the application of the Fourier projection slice theorem in conjunction with the Fourier technique of solving the scalar wave equations. Briefly the Fourier projection slice theorem states that the one-dimensional transform

$$W(k_x) = \int_{-\infty}^{\infty} w(x) \exp(ik_x x) \, dx \tag{2}$$

of the projection $w(x)$, defined as

$$w(x) = \int_{-\infty}^{\infty} f(x, y) \, dy \tag{3}$$

is equivalent to the two-dimensional Fourier transform $F(k_x, k_y)$ with $k_y = 0$. In other words it states

$$W(k_x) = F(k_x, k_y = 0). \tag{4}$$

Consequently, a knowledge of a slice of Fourier domain yields $w(x)$ upon the inverse transform. The theorem is to be applied to (1) which is now recognized as the form of a projection integral. Thus the scheme is to find the Fourier slice $P(k_x, k_y = 0; z)$ corresponding to the local value $p(x, y, z)$ of the pressure produced by a given normal particle velocity $u(x, y; z = 0) e^{i\omega t}$ of the transducer; and then numerically compute the inverse transform.

A common method of approaching scalar radiation problems is by resolving the field parameter, i.e., pressure, velocity potential, etc., into a system of plane waves with two-dimensional Fourier transforms. For example, let

$$P(k_x, k_y; z) = \iint p(x, y, z) \exp[-i(k_x x + k_y y)] \, dx \, dy \tag{5}$$

and

$$p(x, y, z) = (\tfrac{1}{2}\pi)^2 \iint P(k_x, k_y; z)$$
$$\cdot \exp[i(k_x x + k_y y)] \, dk_x \, dk_y \tag{6}$$

be a typical transform pair. Here $p(x, y, z)$ is a phasor, as previously defined, that satisfies the Helmholtz equation

$$\nabla^2 p + k^2 p = 0 \tag{7}$$

as in the case of linear nonabsorbing acoustic waves. Substituting (6) into (7), one can obtain

$$\frac{d^2 P}{dz^2} + (k^2 - k_x^2 - k_y^2) P = 0. \tag{8}$$

A solution of (8) is

$$P(k_x, k_y; z) = P(k_x, k_y; z_0) \exp[-ik_z(z - z_0)] \tag{9}$$

where $k_z = (k^2 - k_x^2 - k_y^2)^{1/2}$. Thus, this approach permits calculation of the field in the plane z from a knowledge of the field in the plane z_0. The quantity $P(k_x, k_y; z)$ can be interpreted as the phasor description of plane waves with wave vector (k_x, k_y, k_z). It is noted that k_z can be real, which means that the wave propagates, or imaginary which infers an evanescent wave.

Our intermediate objective is to find $P(k_x, k_y; z)$ from the velocity distribution of the transducer. We started with one component of the force equation

$$\frac{\partial p}{\partial z} = -\rho \frac{\partial u_z}{\partial t} \tag{10a}$$

$$= -i\omega u_z \quad \text{(for harmonic waves)} \tag{10b}$$

where the z axis is in the direction normal to the transducer surface and ρ is the density of the medium. Substituting (9) for the pressure and a similar expression for the particle velocity into (10) one can find

$$P(k_x, k_y; z) = (k/k_z) \rho c \, U_z(k_x, k_y; z) \tag{11}$$

where c is the velocity of sound. Equation (11) is the plane wave relationship between pressure and particle velocity; the term (k/k_z) in the secant of the angle between the direction of propagation of the plane and the z direction when k_z is real.

At this stage of the development, we know how to evaluate $v(x, z)$ from $P(k_x, 0; z)$ and to calculate $P(k_x, 0; z)$ at any plane z from $P(k_x, 0; z_0)$ which are related to a Fourier domain description of the z component of the particle velocity $u_z(k_x, 0; z_0)$. To obtain $u_z(k_x, 0; z_0)$ from the given particle velocity $u_z(x, y, z_0)$, we again apply the Fourier projection slice theorem. We take the projection of $u_z(x, y, z_0)$ to be

$$\overline{U}_z(x, z_0) = \int u_z(x, y, z_0) \, dy \tag{12}$$

where the y direction is chosen to be the direction of light propagation. The one-dimensional transform of $\overline{U}_z(x, z_0)$ is $U_z(k_x, 0; z_0)$ our desired result.

Thus the procedure for calculating the field $v(x, z)$ is as follows.

1) For a given direction of light propagation with respect to transducer geometry, calculate the projection of velocity by (12).
2) Numerically compute the one-dimensional Fourier transform to find $U_z(k_x, 0; z_0)$.
3) Divide by k_z and the other appropriate constants to obtain $P(k_x, 0; z_0)$ as specified by (11).
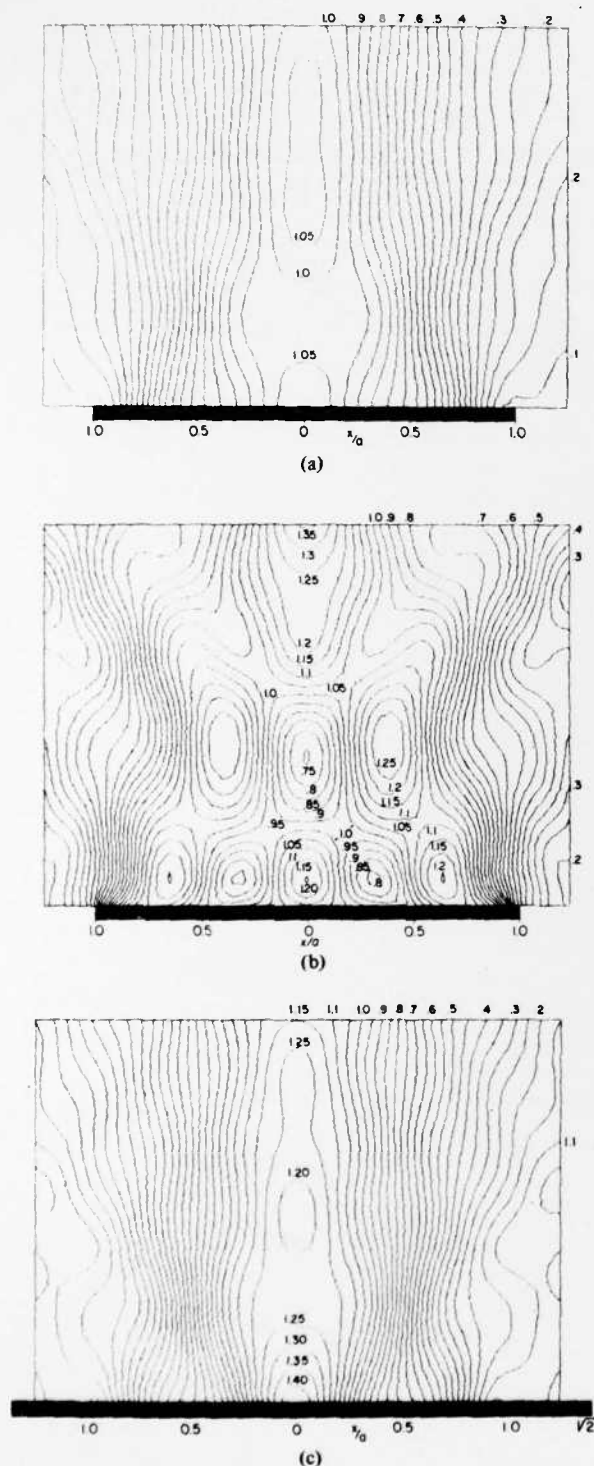4) Calculate $P(k_x, 0; z)$ at desired plane z using (9).

(a)

(b)

(c)

Fig. 3. Computed integrated optical effect (normalized for $ka = 10$.
(a) Circular transducer. (b) Rectangular. (c) Square on diagonal.

5) Compute the inverse one-dimensional transform to
   evaluate $v(x, z)$.

To calculate at alternate distance z from the transducer, re-
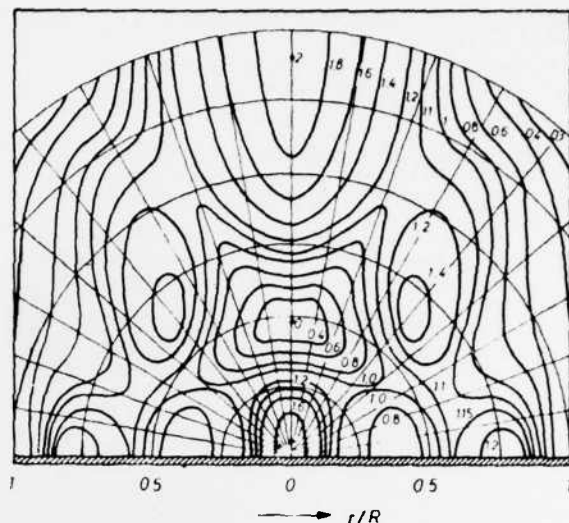peat steps 4) and 5).

Fig. 4. Computed local variation of pressure for a circular piston with
$ka = 10$, from Meyer and Newman [11]. (Courtesy of Academic
Press).

RESULTS

Using the procedure described above we have calculated the
integrated optical effect for a circular, rectangular, and square
transducer on its diagonal with $ka = 10$. The dimension a is
the radius of a circular transducer, half the length of a side of
the square transducer and half the length of the rectangular
transducer perpendicular to the direction of light propagation.
The field variations of $v(x, z)$ for these configurations are
shown in Fig. 3. Assuming the rectangular transducer is square
the normalization $v_0 = 4\pi\kappa a/\lambda$ has been applied for all of these
configurations.

The field variations are observed to be considerably different
in three configurations. The rectangular transducer has the
largest variations, the circular next and the square on the di-
agonal being the most uniform. The results agree with the ob-
servations by Cook and Ingenito [10] and the calculations
along the axis of Ingenito and Cook [3].

The variation in the integrated optical effect are not as large
as the variations in the local value of pressure. Fig. 4 shows
the variation in pressure generated by a circular transducer of
$ka = 10$ for comparison with Fig. 3(a).

Having the field values of $v(x, z)$ allows one to calculate
photographs of schlieren patterns from first principles. To
demonstrate how the transducer geometry and sound level af-
fects the schlieren, we present a series of computed schlieren
patterns. The spatial filter of the schlieren was chosen to pass
only the zeroth diffraction order. The patterns were calcu-
lated by assigning each point in relative intensity
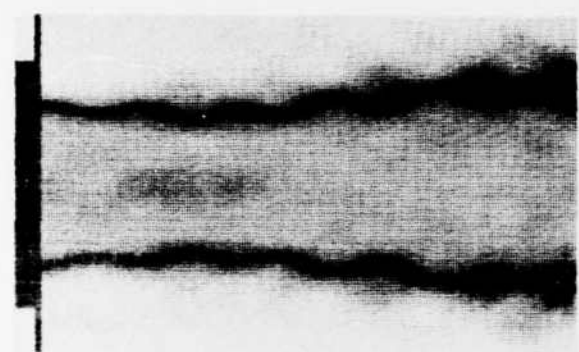
$$I_0 = J_0^2 (v(x, z)) \tag{13}$$

where $J_0(v)$ is the zeroth order Bessel function of the first
kind. A logarithmic response of the film was assumed and a
gray scale assigned. Figs. 5, 6, and 7 correspond to the fields
of Fig. 3(a), 3(b), and 3(c) at various sound levels. In each
case the value of v listed is the maximum value found any-
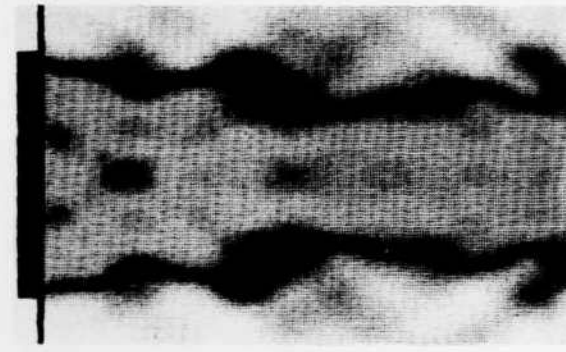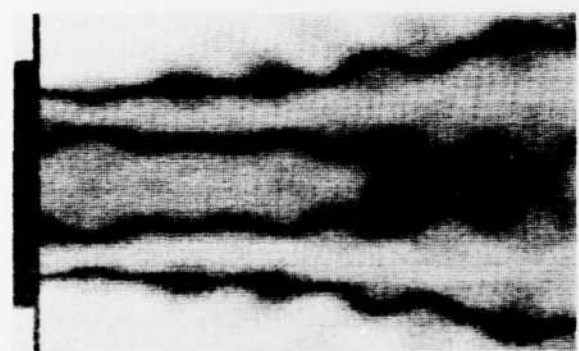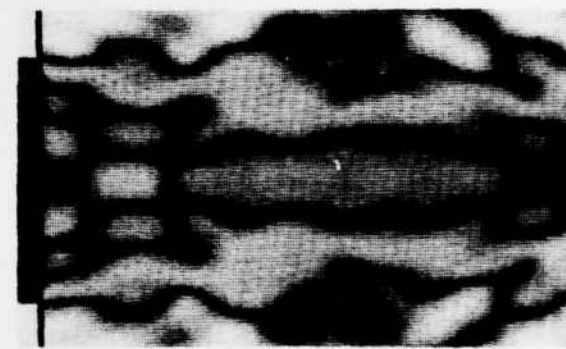where in the field. At low levels, there is a correspondence be-
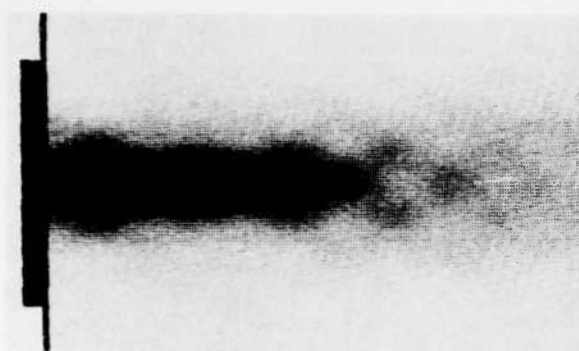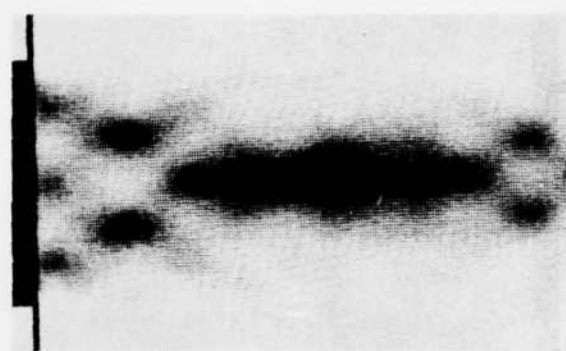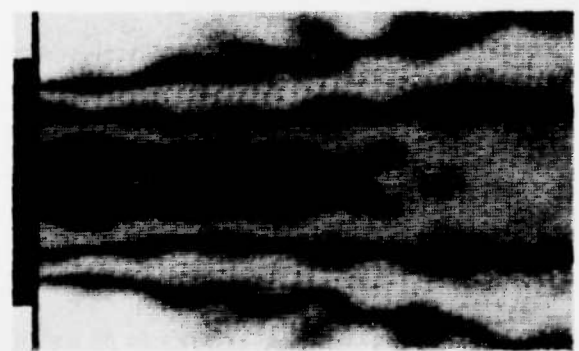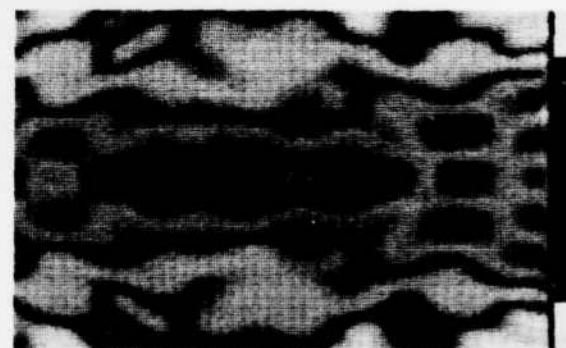
Fig. 5. Computed bright field schlieren for circular transducer at various sound levels. (a) $v = 2.5$. (b) $v = 5.0$. (c) $v = 7.5$. (d) $v = 10.0$.

Fig. 6. Computed bright field schlieren for rectangular transducer at various sound levels. (a) $v = 2.5$. (b) $v = 5.0$. (c) $v = 7.5$. (d) $v = 10.0$.
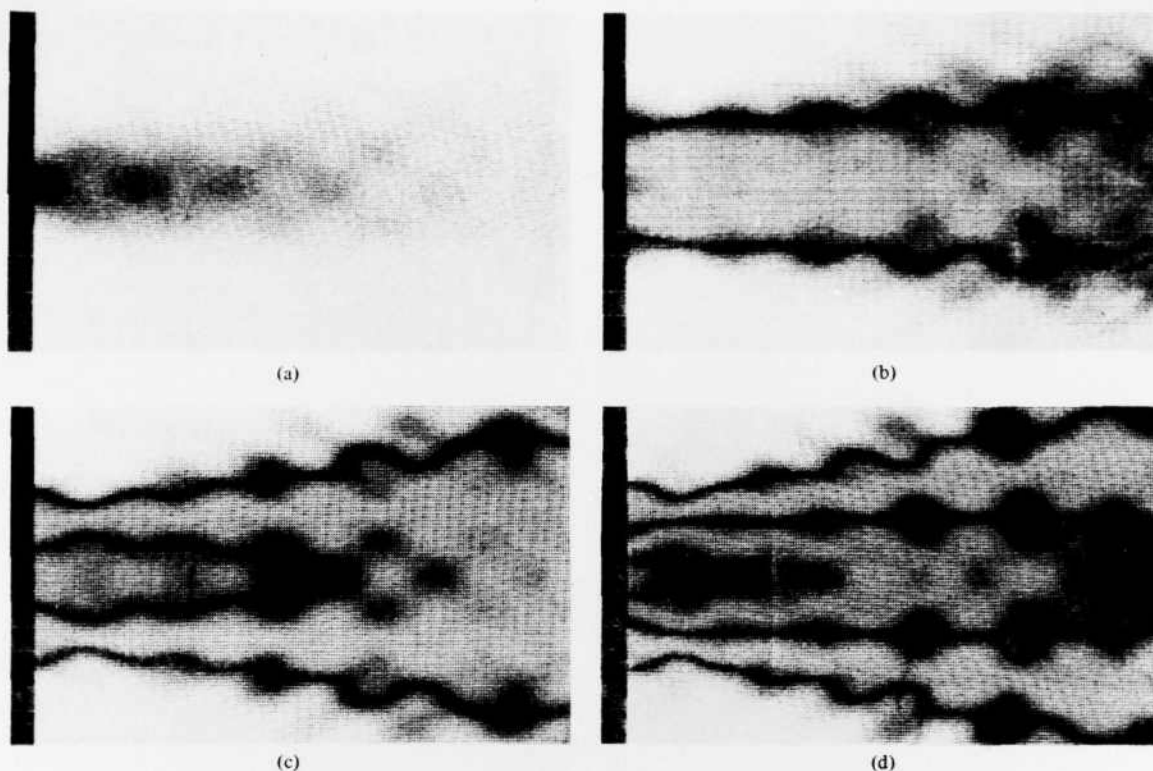
(a)   (b)

(c)   (d)

Fig. 7. Computed bright field schlieren for square transducer on its
diagonal. (a) v = 2.5. (b) v = 5.0. (c) v = 7.5. (d) v = 10.0.
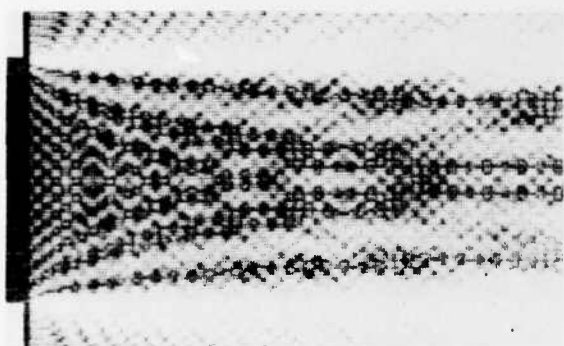

Fig. 8. Computed dark field schlieren approximating the conditions
of Fig. 1 of a square transducer with ka = 45.2.

tween the gray levels and the field value of v in Fig. 3. How-
ever, at higher sound levels, the nonlinear properties of (13)
tends to make the patterns more complicated and less inter-
pretable. However, the spreading nature of the sound beam
becomes more evident at the higher levels.

An increase of ka also changes the pattern. From the de-
scription of Osterhammel's experimental arrangement and an
estimation of the sound level, we have computed the image
shown in Fig. 8 which is to be compared with Fig. 1. As one
can see, many of the geometrical features are duplicated in the
calculated image. In fact, the computed image contains some
gray areas which are in the original photographs but have been
lost in subsequent photographic reproductions. For the pat-

tern shown in Fig. 8, we have chosen a spatial filter that passes
only the first diffraction orders. Consequently, intensity as-
signed to each point is the square of the first-order Bessel func-
tion with the argument v. Other schlieren patterns are shown
elsewhere [11].

CONCLUSION

From first principles it is possible to calculate the integrated
optical effect for any given transducer configuration in the
Raman–Nath region. The numerical technique results from
application for Fourier projection slice theorem and does not
require explicit integration. Implementation via FFT permits
rapid calculations of the integrated optical effect and schlieren
patterns.

This procedure can be adapted easily to other configurations
such as focused transducers, imperfect transducers, zone
plates, and shaded transducers.

ACKNOWLEDGMENT

REFERENCES

[1] K. Osterhammel, "Optische Untersuchung des Schallfeldes
    Kolbenformig Schwinger Quarze," *Akust. Z. Bd. 6*, pp. 73–86,
    1941.
[2] W. R. Klein and B. D. Cook, "Unified approach to ultrasonic

light diffraction," *IEEE Trans. Sonics Ultrason.*, vol. SU-14, pp. 123–134, 1967.

[3] F. Ingenito and B. D. Cook, "Theoretical investigation of the integrated optical effect produced by sound fields radiated from plane piston transducer," *J. Acoust. Soc. Am.*, vol. 45, pp. 572–577, 1969.

[4] W. T. Maloney, G. Meltz, and R. L. Gravel, "Optical probing of the Frensel and Fraunhofer regions of a rectangular acoustic transducer," *IEEE Trans. Sonics Ultrason.*, vol. SU-15, pp. 167–172, 1968.

[5] A. J. Crandal, "Measurement of the velocity of sound in water by optical methods," Ph.D. thesis, Department of Physics, Michigan State University, East Lansing, University Microfilms No. 68-7882.

[6] M. E. Haran, B. D. Cook, and H. F. Stewart, "Comparison of an acoustooptic and a radiation force method of measuring ultrasonic power," *J. Acoust. Soc. Am.*, vol. 57, pp. 1436–1440, 1975.

[7] R. Riebold, W. Molkenstruck, and K. M. Swamy, "Experimental study of the integrated optical effect of ultrasonic fields," *Acustica*, vol. 43, pp. 253–259, 1979.

[8] R. Riebold, "The measurement of ultrasonic power using an acousto-optic method," *Acustica*, vol. 36, pp. 214–220, 1976/1977.

[9] J. C. Berlinghieri and B. D. Cook, "Data requirements for mapping of ultrasonic fields with conventional light diffraction," *J. Acoust. Soc. Am.*, vol. 58, pp. 823–827, 1975.

[10] B. D. Cook and F. Ingenito, "Ultrasonic transducer configuration for producing a phase grating of nearly uniform strength," *Proc. IEEE*, vol. 56, pp. 871–872, 1968.

[11] B. D. Cook, "A procedure for calculating the integrated acoustooptic (Raman–Nath) parameter for the entire sound field," presented at the 1979 Ultrasonic Symp., New Orleans, LA, Sept. 26–28, 1979, paper p-8.

[12] E. Meyer and E. Newman, *Physical and Applied Acoustics: An Introduction.* New York and London: Academic, 1972, p. 175.

A PROCEDURE FOR CALCULATING THE INTEGRATED ACOUSTO-OPTIC (RAMAN-NATH) PARAMETER FOR THE ENTIRE SOUND FIELD

β

BILL D. COOK

Cullen College of Engineering
University of Houston Central Campus, Houston, Texas   77004

ABSTRACT

An important parameter in acousto-optics is the so-called Raman-Nath parameter which measures the integrated change of optical path produced by an ultrasonic field. A straight-forward procedure has been developed for calculating this parameter for the entire sound field for an arbitrary velocity profile and arbitrary configuration of a baffled planer transducer. Examples will be shown for the square transducer. The technique is limited to linear acoustics and the Raman-Nath region of acousto-optics interaction.

Figure 1 shows the basic optical arrangement for visualizing ultrasonic fields. The type of spatial filtering performed in plane P_3 dictates the type of pattern seen in the image plane P_4. Most common types of filter choices are the following:

1. Pass only the zeroth order
2. Block only the zeroth order
3. Pass only the first diffraction order

However, the complexity seen in the Schleiren pattern depends on the soundfield and the integration of the optical effect through this field. Figure 2 shows the complexity that can occur in the photograph. In this case, the transducer is rectangular and supposedly moving as a piston. In this paper, we demonstrate that these patterns can be theoretically predicted by modeling the configuration and movement of transducer, the optical integration over the resultant sound field and the spatial filtering. The mathematical details of implementing these calculations are outlined elsewhere[1]. However, it should be noted here that the procedure for calculating the integrated

optical effect is rapid as it is implemented by applying the fast fourier transform algorithms and has no integration as given in other techniques[2,3].

Basically, it involves taking the projection of transducer velocity in the direction of light propagation; taking the fourier transform, dividing by the cosine of the angles of plane wave assigned to resultant transform variable[4], accounting for propagation with a phase term and taking the inverse fourier transform. As these are one dimensional transforms, one can calculate the field with close spacing without excess cost.

In the calculations shown, we have applied simple spatial filtering typically done [5]. An arbitrary choice for photographic film response has been included to yield a balance of the gray tones.

Figure 2 is taken from a 1941 paper by Osterhammel[6]. From the parameter given and trial and error estimation of the sound level, we show Figure 3 as an example of the calculation. Many features shown in Osterhammel's photograph are reproduced in our computer results.

A demonstration of the effect of the direction of light propagation to sound field has previously been published[7]. It is duplicated in Figure 4. The light is propagating with respect to the orientation of a square transducer as illustrated. Figure 5 shows the result of calculations with the same orientation but with a different ka.

References

[1]B.D. Cook and E. Cavanagh, submitted to IEEE Trans. Sonics Ultrasonics.

[2]W.T. Maloney, G. Meltz, and R. Gravel, IEEE Trans. Sonics Ultrasonics SU-15, 167-172 (1968).

[3]E. Ingenito and B.D. Cook, J. Acoust. Soc. Am. 45 572-577, (1969).

[4]J.W. Goodman, Introduction to Fourier Optics, (McGraw-Hill, San Francisco 1968) p. 50.

[5]W.E. Moore and J.A. Bucaro, J. Acoust. Soc. Am. 63 60-67, (1978).

[6]K. Osterhammel, Ahust, Z. Bd. 6, 73-86, (1941).

[7]B.D. Cook and E. Ingenito, Proc. IEEE 56 871-872 (1968).

Dr. Bill D. Cook
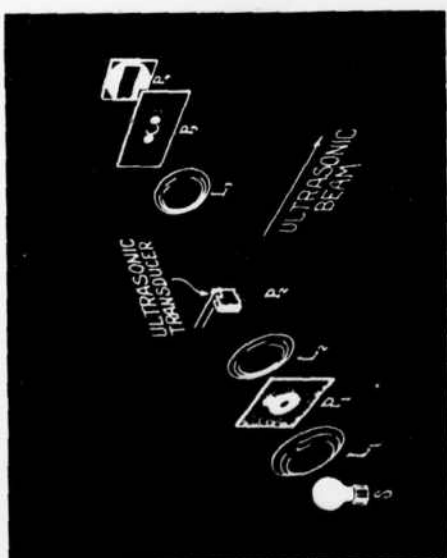

Figure 1. left- Optical arrangement for Schlieren.

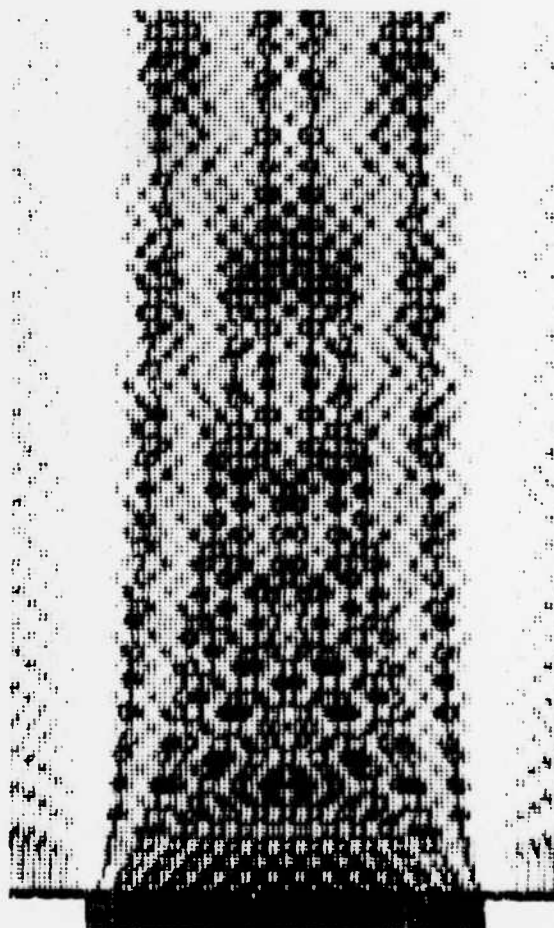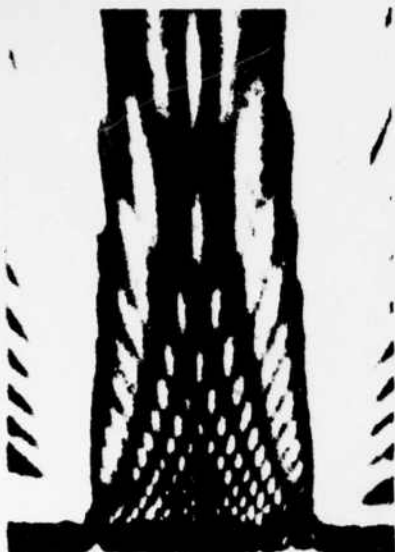Figure 2. right- Schlieren photograph with first order passed. Rectangular transducer, ka = 45.2.

Figure 3. left- Computer generated Schlieren pattern for parameters given in Figure 2.

Dr. Bill D. Cook

(a)

(b)

Figure 4. Demonstrated effect of direction of light propagation through the sound field produced by a square transducer.
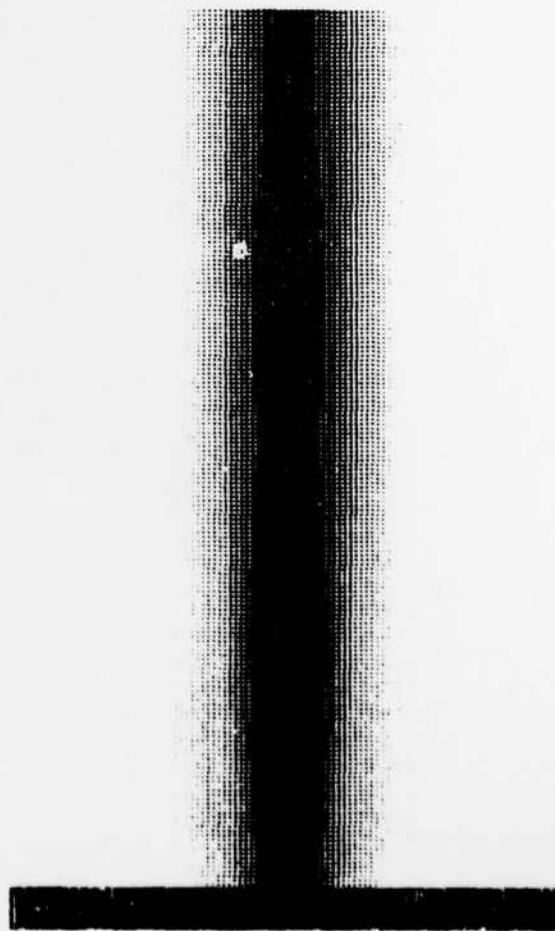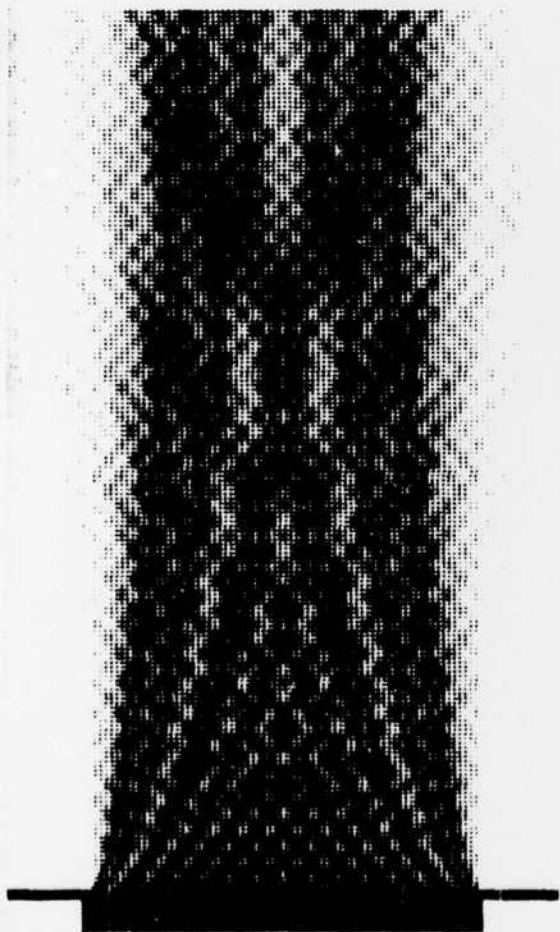
Dr. Bill D. Cook

Figure 5. Computer generated Schlieren for parameters of Figure 4, a and b respectively.

Comparison of the experimental and theoretical pressure fields in the nearfield of ultrasonic transducer-lens systems

P. L. Edwards[a]

The University of West Florida, Pensacola, Florida 32504

Bill D. Cook[a]

Cullen College of Engineering, University of Houston, Central Campus, Houston, Texas 77004

Henry D. Dardy

U. S. Naval Research Laboratory, Washington, D. C. 20375

Experimental measurements of acoustic pressure fields near the focal points of ultrasonic transducer-lens systems are compared to calculations of a recently developed analytic technique. This method incorporates the Fresnel approximation to expand the field in terms of Gaussian-Laguerre functions to calculate the acoustic field for arbitrary placement of a lens in the nearfield of a circular transducer. The predicted field pattern symmetries near the focal region with a lens located either at one focal distance or at the transducer face are confirmed by experimental measurements made with a microsphere probe.

PACS numbers: 43.20.Rz

Recently reported results of Cavanagh and Cook[1,2] establish a method for calculating the acoustic pressure fields in circular ultrasonic transducer-lens systems. Unlike other techniques, this method permits the determination of pressure fields when a lens is placed at an arbitrary position on axis in the nearfield of a circular piston transducer. These calculations indicate that significant spatial field changes occur in the focal region when the position of the lens shifts. In particular, they predict spatial symmetry of the field about the focal plane when the lens is placed on focal length from the transducer; similarly, with the lens located at the surface of the transducer, they predict a pressure maximum shifted towards the transducer rather than at the geometric focal point. This last feature is a known fact of physical optics and has been confirmed experimentally many times.
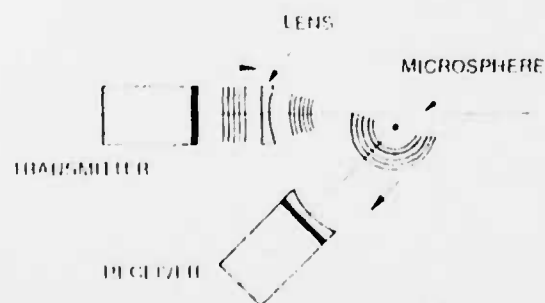

FIG. 1. Experimental apparatus for measurement of pressure field. The microsphere and receiver remain at a fixed position while the source field is processed through their viewing window.
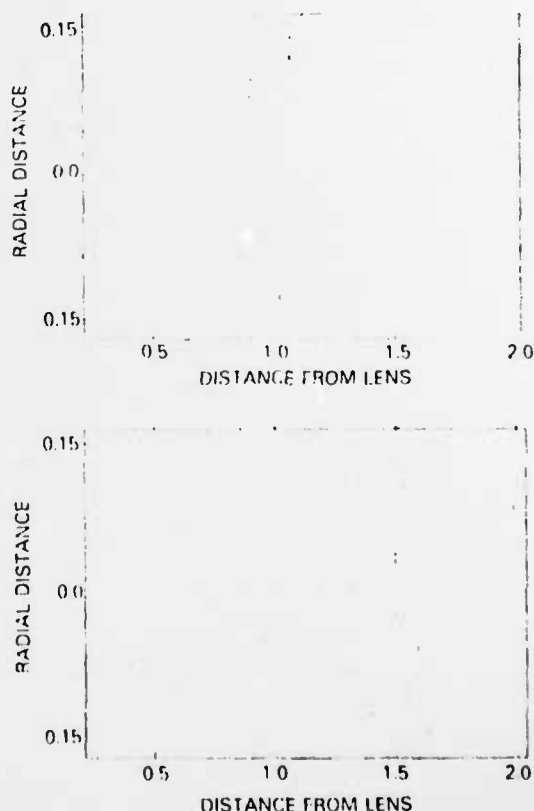

FIG. 2. Calculated pressure field for lens mounted at transducer face (upper) and at one focal distance from the transducer face (lower). Dimensions are in inches.
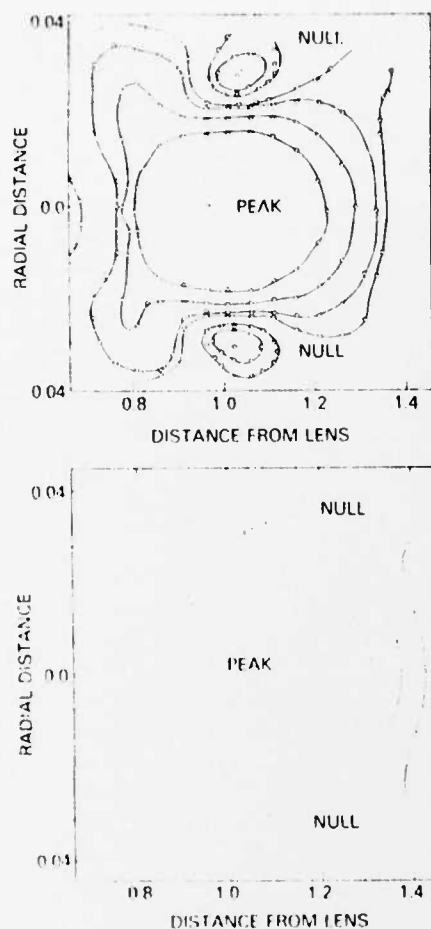
RADIAL DISTANCE

0.04

0.0

0.04

PEAK

NULL

NULL

0.8 1.0 1.2 1.4

DISTANCE FROM LENS

RADIAL DISTANCE

0.04

0.0

0.04

PEAK

NULL

NULL

0.8 1.0 1.2 1.4

DISTANCE FROM LENS

FIG. 3. Experimentally measured (upper) and calculated (lower) pressure contours for lens mounted at transducer face.

RADIAL DISTANCE

0.04

0.0

0.04

PEAK

NULL

NULL

0.6 0.8 1.0 1.2 1.4

DISTANCE FROM LENS

RADIAL DISTANCE

0.04

0.0

0.04

PEAK

NULL

NULL

0.6 0.8 1.0 1.2 1.4

DISTANCE FROM LENS

FIG. 4. Experimentally measured (upper) and computed (lower) pressure contours for lens mounted at one focal distance from transducer face.

Experimentally measured values are here compared with calculated values of the field in the region near the focal point for a circular transducer of 0.5 in. diam operating at a frequency of 5.0 MHz. A lucite lens with a focal length of 1 in. was placed coaxially both at the transducer face and at one focal distance from the transducer face. The resulting pressure field was measured by moving a microsphere in rasterlike fashion through the focal region; the technique, developed by Edwards and Jarzynski, [?] utilizes the amplitude of the scattered wave as a measure of the field strength at the microsphere location (Fig. 1). In this arrangement, the microsphere is positioned at the focal point of the receiver and both are held at a fixed position during the course of the experiment. The transmitter and lens system is positioned so that the microsphere interrogates the desired region of the pressure field. The microsphere has a radius of approximately 0.001 in., sufficiently small so that even the focused field presents essentially a uniform field over the area of the sphere. At 5.0 MHz, the product of wavenumber and diameter, ka, is approximately 0.5. The amplitude of the scattered wave is therefore relatively independent of the scattering
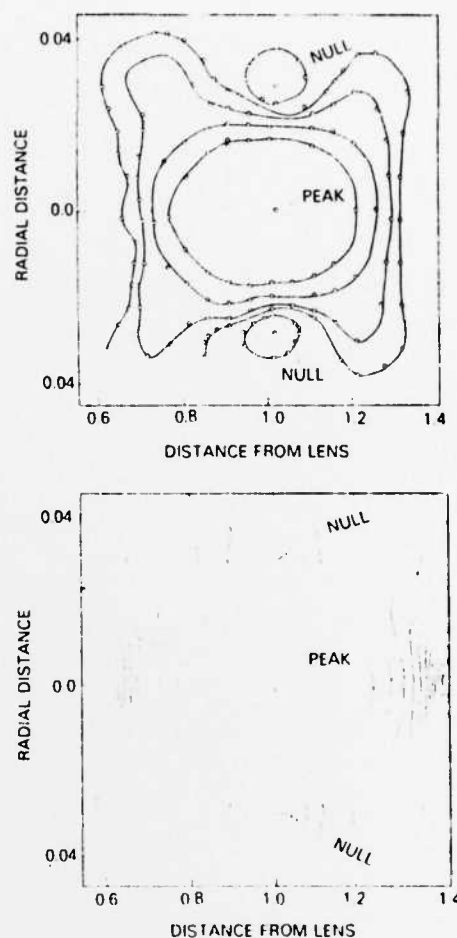
$P_{Q_{MAX}}$ 1.0 0.5 0.0

0.6 1.0 1.4 1.8

1.0 0.5 0.0

0.6 1.0 1.4 1.8

$P_{P_{MAX}}$ 1.0 0.5 0.0

0.6 1.0 1.4 1.8

DISTANCE FROM LENS

1.0 0.5 0.0
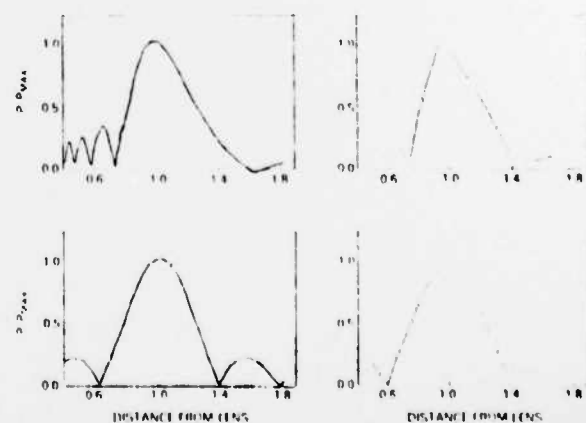
0.6 1.0 1.4 1.8

DISTANCE FROM LENS

FIG. 5. Comparison of pressure on transducer axis through focal region, computed for lens on transducer face (upper left), measured with lens on face (upper right), computed with lens at one focal distance (lower left), and measured with lens at one focal distance (lower right).
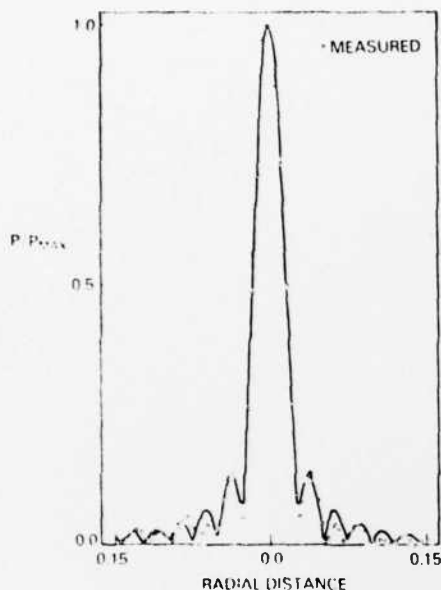
FIG. 5. Measured (·) and computer (-) pressure in the plane perpendicular to the transmitter axis at the point where the axial pressure is a maximum for the case where the lens is mounted on the transducer face.

angles encountered in the experiment.

Figure 2 illustrates the calculated fields for the two transducer-lens geometries. The top diagram illustrates the field obtained for the lens positioned at the transducer face; the same pattern can be expected for the situation of a transducer with a curved radiating surface. The lower diagram, for the lens positioned at one focal length, indicates a significant structural change occurs under these circumstances. In both cases, the abscissa measures the distance from the lens and the ordinate has been expanded to show the resultant spatial detail. Minor differences in the high degree of symmetry exhibited in the lower of the plots is a result of the computer graphic contour routine and not of the analytic development; in both instances the pressure peak in the diagrams is normalized to 0.0 dB and the contours chosen to map 3.0-dB intervals. The experimental and calculated values shown in the remaining figures expand only the central region of these detailed plots.

Measured and computed pressure profiles for the case where the lens is mounted at the transducer face are given in Fig. 3. The measured contour structure in this case is in good agreement with the predicted

values; the expanded scale of presentation allows verification of the location of the pressure peaks and nulls. In both diagrams, the contour nearest the peak is − 6.0 dB relative to the peak pressure; the remaining intervals are − 3.0 dB down (i.e., − 9.0 dB, − 12.0 dB, etc.). There is an experimental error of approximately 1.0 dB due to the nonlinear response of the measuring electronic equipment.

Figure 4 shows the measured and computed contours for the case where the acoustic lens is placed one focal distance from the transducer face. The measured pressure peak and nulls are again in good agreement with that of the calculation; the measured values verify the high degree of symmetry expected. Calculated and experimental pressure profiles along the transducer axis in the region of the pressure peak are shown in Fig. 5. The upper-left curve shows the calculated pressure for a lens mounted on the source face, the upper right shows the experimentally measured pressure. The lower curves repeat the process for the lens located at the focal distance. The calculated pressure curve in the plane perpendicular to the axis at the point of maximum axial pressure, a distance of approximately 0.96 in. from the lens, is plotted in Fig. 6, along with the experimentally measured values.

Experimental evidence indicates that the method of Cavanagh and Cook adequately predicts the pressure field of ultrasonic transducer-lens system. Calculations, performed point for point with the Gaussian-Laguerre algorithm, allow for quick computation. The results outlined in this work assume the lens large compared to the width of the sound beam. The analytic formulation has been extended to predict the field for finite size lenses. Additionally, the experimental evidence presented indicates the utility of the microsphere probe to spatially map with high resolution and precision the fields encounter in focused ultrasound.

[1] E. Cavanagh and B. D. Cook, "Nearfield of Ultrasonic Transducer-Lens Systems: Theory of the Gaussian-Laguerre Formulation," J. Acoust. Soc. Am. Suppl. 1 66, S46 (1979).

[2] E. Cavanagh and B. D. Cook, "Description of Ultrasonic Fields Using Gaussian-Laguerre Formulation. Numerical Example: Circular Piston," J. Acoust. Soc. Am. 68, 1136–1140 (1980).
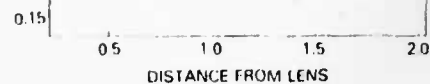
[3] P. L. Edwards and J. Jarzynski, "Experimental and Theoretical Study of the Scattering of Focused Ultrasound from Microparticles in Fluids," J. Acoust. Soc. Am. Suppl. 1 65, S128 (1979).

[4] P. L. Edwards and J. Jarzynski, "Use of a Microsphere Probe for Pressure Field Measurements in the Megahertz Frequency Range," J. Acoust. Soc. Am. 68, 356–358 (1980).

DATE
ILME

DISTANCE FROM LENS

FIG. 2. Calculated pressure field for lens mounted at transducer face (upper) and at one focal distance from the transducer face (lower). Dimensions are in inches.

of the experiment. The transmitter and lens system is
positioned so that the microsphere interrogates the
desired region of the pressure field. The microsphere
has a radius of approximately 0.001 in., sufficiently
small so that even the focused field presents essentially
a uniform field over the area of the sphere. At 5.0
MHz, the product of waveconstant and diameter, ka, is
approximately 0.5. The amplitude of the scattered wave
is therefore relatively independent of the scattering

FIG. 5. Comparison of pressure on transducer axis through
focal region, computed for lens on transducer face (upper
left), measured with lens on face (upper right), computed with
lens at one focal distance (lower left), and measured with lens
at one focal distance (lower right).